



HAL
open science

The low energy spectrum of finite size metallic SWNTs

Leonhard Mayrhofer, Milena Grifoni

► **To cite this version:**

Leonhard Mayrhofer, Milena Grifoni. The low energy spectrum of finite size metallic SWNTs. The European Physical Journal B: Condensed Matter and Complex Systems, 2008, 63, pp.43-58. 10.1140/epjb/e2008-00204-0 . hal-00166887

HAL Id: hal-00166887

<https://hal.science/hal-00166887>

Submitted on 10 Aug 2007

HAL is a multi-disciplinary open access archive for the deposit and dissemination of scientific research documents, whether they are published or not. The documents may come from teaching and research institutions in France or abroad, or from public or private research centers.

L'archive ouverte pluridisciplinaire **HAL**, est destinée au dépôt et à la diffusion de documents scientifiques de niveau recherche, publiés ou non, émanant des établissements d'enseignement et de recherche français ou étrangers, des laboratoires publics ou privés.

The low energy spectrum of finite size metallic SWNTs

Leonhard Mayrhofer and Milena Grifoni
Theoretische Physik, Universität Regensburg, 93040 Germany
(Dated: 10th August 2007)

The electronic spectrum of metallic finite-size single-wall carbon nanotubes at low energies is derived. It is based on a tight-binding description for the interacting p_z electrons. Not only the forward scattering parts of the Coulomb interaction, which are diagonalized by bosonization, are considered, but also all other processes becoming relevant for small diameter tubes. As a consequence of the substructure of the underlying lattice, a spin 1 triplet is found as ground state if the exchange splitting is larger than the branch mismatch, a spin 0 singlet otherwise. Moreover the excitation spectrum is calculated.

PACS numbers: 73.63.Fg, 71.10.Pm, 71.70.Gm, 73.23.Hk

Single-walled carbon nanotubes (SWNTs) are one of the most prominent examples for the realization of 1D electronic systems with orbital degeneracy in nature. A proper description of the low energy regime has to take into account the Coulomb interaction between the electrons and the corresponding correlation effects. Luttinger Liquid behaviour, leading to power-law dependence of various transport quantities, has been predicted theoretically for metallic SWNTs of infinite length [1, 2] and was confirmed experimentally [3, 4]. Considering tubes of finite length, Kane et al. [5] have derived the discrete energy spectrum of the collective spin and charge excitations and its dependence on the forward scattering part of the Coulomb interaction. Moreover, for SWNTs a charging energy of the order of the level spacing is found, leading to the observation of Coulomb blockade in SWNT quantum dot devices [6, 7, 8, 9, 10]. The accompanying two- or fourfold periodicity of the Coulomb diamond size can be understood by including the spin and band degrees of freedom. A theory of transport through SWNT quantum dots incorporating the mentioned forward scattering interaction processes was worked out in [11]. As discussed below, the restriction to forward scattering terms is justified for large diameter tubes only, whereas the remaining interaction processes become more and more important for decreasing tube diameters. They lead to exchange effects and a modification of the excitation spectrum. Within a meanfield approach Oreg et al. [12] predicted exchange effects favouring spin alignment. The size of the exchange splitting on the SWNT ground states was measured by recent experiments [8, 9, 10].

A fundamental question regards the nature of the ground state and excited spectrum of correlated 1D systems. In a milestone theorem Lieb and Mattis [13] demonstrated that for a 1D Hubbard model with nearest neighbour hopping, the ground state must have spin 0 or 1/2. They left open the question for systems with orbital degeneracy. This is the case for SWNTs due to the substructure of the underlying honeycomb lattice.

In this work we go beyond the mean field approach and derive the electronic structure of metallic SWNTs in

the low energy regime from a microscopic model. Beside the long ranged forward scattering terms of the Coulomb interaction, which are exactly diagonalized by bosonization, we take into account *all* other processes becoming relevant for small diameter SWNTs away from half-filling. Because of scattering processes involving the orbital degree of freedom, we predict a spin 1 triplet as ground state, if the exchange energy exceeds the energy mismatch between the two electron branches and if $4m + 2$ electrons occupy the SWNT. Moreover the excitation spectra are calculated. The large degeneracies of the discrete energy levels, as obtained by only including forward scattering terms, are partly lifted and the spectra become quasi-continuous when going to higher energies.

The low energy Hamiltonian of metallic finite size SWNTs Without loss of generality we focus on armchair SWNTs [14]. As basis of our future discussion let us recall the minimal model Hamiltonian to describe finite size armchair SWNTs at low energies derived in [11]. It is based on p_z electrons localized on the graphene honeycomb lattice which contains two carbon atoms, $p = \pm$, per unit cell. Let the SWNT axis be along the x direction and ignore for the moment interactions. Then, by imposing periodic boundary conditions along the circumference and open ones along the tube length, eigenfunctions are standing waves $\varphi_{r\kappa}(\vec{r})$ with the branch or pseudo-spin index $r = \pm$. The wave number κ describes the slowly varying oscillations of $\varphi_{r\kappa}(\vec{r})$. The finite tube length L leads to the quantization condition $\kappa = \pi(m_\kappa + \Delta)/L$, $m_\kappa \in \mathbb{Z}$, $|\Delta| \leq 1/2$. The parameter Δ is responsible for a possible energy mismatch between the branches $r = \pm$; its value depends on the length and on the type of the considered SWNT [15]. Explicitly, $\varphi_{r\kappa}(\vec{r})$ can be decomposed into its contributions from the sublattices $p = \pm$, $\varphi_{r\kappa}(\vec{r}) = \frac{1}{\sqrt{2}} \sum_{p=\pm} f_{pr} \sum_{F=\pm K_0} \text{sgn}(F) e^{i \text{sgn}(F) \kappa x} \varphi_{pF}(\vec{r})$, where $f_{+r} = 1/\sqrt{2}$ and $f_{-r} = -r/\sqrt{2}$. The functions $\varphi_{pF}(\vec{r})$ describe fast oscillating Bloch waves at the two independent Fermi points $F = \pm K_0$ of the honeycomb lattice, $\varphi_{pF}(\vec{r}) = N_L^{-1/2} \sum_{\vec{R}} e^{iF R_x} \chi(\vec{r} - \vec{R} - \vec{\tau}_p)$, where

$\chi(\vec{r} - \vec{R} - \vec{\tau}_p)$ is the p_z orbital at lattice site \vec{R} on sublattice p and N_L is the total number of lattice sites. The non-interacting Hamiltonian then reads

$$H_0 = \hbar v_F \sum_{r\sigma} r \sum_{\kappa} \kappa c_{r\sigma\kappa}^\dagger c_{r\sigma\kappa},$$

where $v_F \approx 8.1 \cdot 10^5$ m/s is the Fermi velocity of graphene and $c_{r\sigma\kappa}$ annihilates an electron in the state $|\varphi_{r\kappa}\rangle_{|\sigma\rangle}$. Introducing the slowly varying 1D operators $\psi_{r\sigma F}(x)$ [11] defined along the tube axis,

$$\psi_{r\sigma F}(x) = \frac{1}{\sqrt{2L}} \sum_{\kappa} e^{i\text{sgn}(F)\kappa x} c_{r\sigma\kappa}, \quad (1)$$

and integrating over the coordinates perpendicular to the tube axis, the interaction part of the Hamiltonian becomes effectively one dimensional. We find

$$V = \frac{1}{2} \sum_{\sigma\sigma'} \sum_{\{[r],[F]\}} \prod_{i=1}^4 \text{sgn}(F_i) \int \int dx dx' U_{[r][F]}(x, x') \times \psi_{r_1\sigma F_1}^\dagger(x) \psi_{r_2\sigma' F_2}^\dagger(x') \psi_{r_3\sigma' F_3}(x') \psi_{r_4\sigma F_4}(x). \quad (2)$$

Here $\sum_{\{[r],[F]\}}$ denotes the sum over all quadruples $[r] = (r_1, r_2, r_3, r_4)$ and $[F] = (F_1, F_2, F_3, F_4)$. Assuming that the wave functions $\varphi_{p,F}(\vec{r})$ and $\varphi_{-p,F}(\vec{r})$ do not overlap, the effective 1D Coulomb interaction potential

$$U_{[r][F]}(x, x') = \frac{1}{4} \left[U_{[F]}^{\text{intra}}(x, x') (1 + r_1 r_2 r_3 r_4) + U_{[F]}^{\text{inter}}(x, x') (r_2 r_3 + r_1 r_4) \right], \quad (3)$$

can be separated into an interaction for electrons on the same (intra) and on different sublattices (inter), where

$$U_{[F]}^{\text{intra/inter}}(x, x') = L^2 \int \int d^2 r_\perp d^2 r'_\perp \times \varphi_{pF_1}^*(\vec{r}) \varphi_{\pm p F_2}^*(\vec{r}') \varphi_{\pm p F_3}(\vec{r}') \varphi_{p F_4}(\vec{r}) U(\vec{r} - \vec{r}'),$$

and $U(\vec{r} - \vec{r}')$ is the Coulomb potential. For the actual calculations we model $U(\vec{r} - \vec{r}')$ by the so called Ohno potential. Measuring distances in units of \AA and energy in eV, it is given by $U(\vec{r} - \vec{r}') = U_0 / \sqrt{1 + (U_0 \epsilon |\vec{r} - \vec{r}'| / 14.397)^2}$ eV [16]. A reasonable choice is $U_0 = 15$ eV [12]. The dielectric constant is given by $\epsilon \approx 1.4 - 2.4$ [1].

The relevant scattering processes To proceed, it is convenient to introduce the notion of forward (f)-, back (b)-, and Umklapp (u)- scattering for an arbitrary index quadruple $[I]$ associated to the four electron operators in (2). With S_I being the type of scattering process for the quantity I , we denote a quadruple $[I, \pm I, \pm I, I]$ by $[I]_{S_I=f\pm}$, while $[I]_b$ is equivalent to $[I, -I, I, -I]$. Finally Umklapp scattering means $[I]_u =$

$[I, I, -I, -I]$. As we will show in the sequel the interaction part V of the Hamiltonian is of the form $V = \sum_{S_r=f,b,u} \sum_{S_F=f,b} \sum_{S_\sigma=f} V_{S_r S_F S_\sigma}$, where

$$V_{S_r S_F S_\sigma} := \frac{1}{2} \sum_{\{[r]_{S_r}, [F]_{S_F}, [\sigma]_{S_\sigma}\}} \int \int dx dx' U_{[r][F]}(x, x') \times \psi_{r_1\sigma F_1}^\dagger(x) \psi_{r_2\sigma' F_2}^\dagger(x') \psi_{r_3\sigma' F_3}(x') \psi_{r_4\sigma F_4}(x). \quad (4)$$

We start with the S_r scattering types. From (3) it is evident, that the effective interaction potential is only nonzero for $r_2 r_3 = r_1 r_4$. Hence we have to distinguish between the following two cases,

$$a) r_1 = r_4, r_2 = r_3 \text{ and } b) r_1 = -r_4, r_2 = -r_3.$$

In case a) we have $S_r = f$ and $U_{[r]_f[F]}(x, x')$ is the sum of intra- and inter- lattice interaction. Case b) comprises $S_r = b$ and $S_r = u$, with $U_{[r]_{b/u}[F]}(x, x')$ being the difference of the two types of sublattice interactions. Now we look at the allowed S_F processes. Although not dealing with an infinite system, after the integrations along the tube axis in (2), only terms with $F_1 + F_2 - F_3 - F_4 = 0$, i.e. the $S_F = f$ and $S_F = b$ processes, dominate as a consequence of the approximate conservation of quasi momentum. All other processes, including $S_F = u$, have very small amplitudes. Finally, regarding the spin index, only $S_\sigma = f$ terms are allowed, since the Coulomb interaction is spin independent.

Additionally, away from half filling, only terms with $r_1 F_1 + r_2 F_2 - r_3 F_3 - r_4 F_4 = 0$ are relevant in (2), due to conservation of the quasi momentum, arising from the slow oscillations of the 1D electron operators.

Since $U_{[F]}^{\text{intra}}$ and $U_{[F]}^{\text{inter}}$ differ only at the length scale of the lattice spacing [1], the interaction potential for case b) ($\rightarrow S_r = b, u$) is generally short ranged compared to the slowly varying electron operators $\psi_{r\sigma F}$, whereas in case a) ($\rightarrow S_r = f$), this is only true for the $S_F = b$ terms. Hence for $S_r = b, u$ or $S_F = b$ the corresponding interactions become effectively local:

$$V_{S_r S_F S_\sigma} := L u^{S_r S_F} \sum_{\{[r]_{S_r}, [F]_{S_F}, [\sigma]_{S_\sigma}\}} \times \int_0^L dx \psi_{r_1\sigma F_1}^\dagger(x) \psi_{r_2\sigma' F_2}^\dagger(x) \psi_{r_3\sigma' F_3}(x) \psi_{r_4\sigma F_4}(x), \quad (5)$$

where the coupling constants are given by $u^{S_r S_F} = 1 / (2L^2) \int \int dx dx' U_{[r]_{S_r}, [F]_{S_F}}(x, x')$. It holds $u^{b S_F} = u^{u S_F} =: u^{\Delta S_F}$ and we define $u^+ := u^{f b}$. The ratio $u^{S_r S_F} / \epsilon_0$ is independent of L but scales like $1/d$ where d is the tube diameter, such that these processes become negligible for large diameter tubes. Numerically we find $u^+ \approx u^{\Delta b} = 0.22 [0.28] \frac{\epsilon_0}{d} \text{\AA}$ and $u^{\Delta f} = 0.14 [0.22] \frac{\epsilon_0}{d} \text{\AA}$ for $\epsilon = 1.4$ [2.4].

Density-density interactions In the next step we introduce the quantities $V_{\rho\rho}$ and $V_{n\rho\rho}$ that collect all interaction processes that are of density-density and non-density-density form, respectively, such that in total $H = H_0 + V_{\rho\rho} + V_{n\rho\rho}$. Since the short ranged interactions are treated as local, we obtain

$$V_{\rho\rho} := V_{f f f} + V_{f^+ b f^+} + V_{b f^+ / b f^+},$$

where the dominating part of the interaction away from half filling is the long-ranged term $V_{f f f}$. Using bosonization techniques [17], the Hamiltonian $H_0 + V_{\rho\rho}$ can be diagonalized and we find

$$H_0 + V_{\rho\rho} = \sum_{j\delta} \sum_{q>0} \varepsilon_{j\delta q} a_{j\delta q}^\dagger a_{j\delta q} + \frac{1}{2} E_c \mathcal{N}_c^2 + \frac{1}{2} \sum_{r\sigma} \mathcal{N}_{r\sigma} \left[\mathcal{N}_{r\sigma} (\varepsilon_0 - u^+) + r\varepsilon_\Delta - \frac{J}{2} \mathcal{N}_{-r\sigma} \right], \quad (6)$$

where we have defined $J := 2(u^{\Delta f} + u^{\Delta b})$. The first term describes discrete excitations created/annihilated by the bosonic operators $a_{j\delta q}/a_{j\delta q}^\dagger$. The four channels $j\delta = c+, c-, s+, s+$ are related to total and relative (with respect to the r index) charge and spin excitations. With the level spacing of the free electrons, $\varepsilon_0 := \hbar v_F \frac{\pi}{L}$, and $\varepsilon_{0q} := \varepsilon_0 n_q$, $q = n_q \frac{\pi}{L}$ the relations $\varepsilon_{c+q} = \varepsilon_{0q} \sqrt{1 + 8W_q/\varepsilon_0}$, $\varepsilon_{s/c-q} = \varepsilon_{0q} (1 - u^{\Delta b}/\varepsilon_0)$ and $\varepsilon_{s+q} = \varepsilon_{0q} (1 + u^{\Delta b}/\varepsilon_0)$ hold. Due to the dominating $V_{f f f}$ contribution, the ratio $g_q := \varepsilon_{0q}/\varepsilon_{c+q}$ is strongly reduced for small q ($g_q \approx 0.2$) and for large q , g_q tends to 1 [11]. Small corrections due to the coupling constants u^+ and $u^{\Delta f}$ have been omitted. Finally,

$$W_q = \frac{1}{L^2} \int_0^L dx \int_0^L dx' \cos(qx) \cos(qx') U_{[r]_f [F]_f}(x, x').$$

The remaining terms in (6) are fermionic contributions, accounting for the energy cost of changing the number of electrons in the different branches ($r\sigma$). The operators $\mathcal{N}_{r\sigma}$ count the electrons in ($r\sigma$) and $\mathcal{N}_c = \sum_{r\sigma} \mathcal{N}_{r\sigma}$. The single summands account for (in the order of appearance) the Coulomb charging energy $E_c = W_0$, the shell filling energy (because of Pauli's principle), a possible energy mismatch $\varepsilon_\Delta = \text{sgn}(\Delta) \varepsilon_0 \min(2|\Delta|, 2|\Delta| - 1)$ between the r branches if $|\Delta| \neq 0, 1/2$, and a favourable spin alignment of electrons with different r due to $V_{b f^+ / b f^+}$. Note also that the shell filling energy is modified by the attractive contribution $-u^+$ due to $V_{f^+ b f^+}$. The eigenstates of $H_0 + V_{\rho\rho}$ are $|\vec{N}, \vec{m}\rangle := \prod_{j\delta q} (a_{j\delta q}^\dagger)^{m_{n\delta q}} / \sqrt{m_{j\delta q}!} |\vec{N}, 0\rangle$, where $|\vec{N}, 0\rangle$ has no bosonic excitation and $\vec{N} = (N_{-\uparrow}, N_{-\downarrow}, N_{+\uparrow}, N_{+\downarrow})$ defines the number of electrons in each of the branches ($r\sigma$).

Non-density-density processes In the following we concentrate on the situation away from half-filling, where the non-density-density processes $V_{n\rho\rho}$ can be treated as

a small perturbation to the Hamiltonian $H_0 + V_{\rho\rho}$. We calculate the low energy spectrum and the corresponding eigenstates of the full Hamiltonian $H_0 + V_{\rho\rho} + V_{n\rho\rho}$ by evaluating the matrix elements $\langle \vec{N}, \vec{m} | V_{n\rho\rho} | \vec{N}', \vec{m}' \rangle$ and by truncating the Hilbert space at a certain eigenenergy of $H_0 + V_{\rho\rho}$. Near half-filling the strength of $V_{n\rho\rho}$ is highly enhanced and the truncation procedure therefore questionable. We obtain

$$V_{n\rho\rho} = V_{f^+ b f^-} + V_{b f^+ / b f^-} + V_{u f^- / b f}. \quad (7)$$

Low energy spectrum Our truncation scheme to find the low energy spectrum is to only retain the energetically lowest lying states of $H_0 + V_{\rho\rho}$ which have no bosonic excitations. Using (1) and (5), we get for the matrix elements of the contributions on the r.h.s of (7),

$$\begin{aligned} \langle \vec{N}, 0 | V_{S_r S_F S_\sigma} | \vec{N}', 0 \rangle &= \frac{1}{4} u^{S_r S_F} \sum_{\{[r]_{S_r}, [F]_{S_F}, [\sigma]_{FS}\}} \\ &\times \sum_{\kappa_1, \dots, \kappa_4} \langle \vec{N}, 0 | c_{r_1 \sigma \kappa_1}^\dagger c_{r_2 \sigma' \kappa_2}^\dagger c_{r_3 \sigma' \kappa_3} c_{r_4 \sigma \kappa_4} | \vec{N}', 0 \rangle \\ &\times \delta_{\sum_{i=1}^2 \text{sgn}(F_i) \kappa_i - \sum_{i=3}^4 \text{sgn}(F_i) \kappa_i, 0}, \quad (8) \end{aligned}$$

where the Kronecker- δ results from the integration along the tube axis in (5). Note that the states $|\vec{N}, 0\rangle$ are eigenstates of $H_0 + V_{\rho\rho}$ and not of H_0 alone. Hence the evaluation of (8) in general is not straightforward. But for the processes relevant away from half-filling we get the same result and physical insight if we consider for the calculation of (8) $|\vec{N}, 0\rangle$ as the Fermi sea filled up with $N_{r\sigma}$ *noninteracting* electrons in the branch $r\sigma$, i. e. as an eigenstate of H_0 , as we will discuss elsewhere [18].

In the following we focus on the case $N_c = 4m + 2$. As truncated basis we use the states $|\vec{N}, 0\rangle$ with $\vec{N} = (m+1, m+1, m, m)$ and permutations. In the following we denote $|(m+1, m+1, m, m), 0\rangle$ by $|\uparrow\downarrow, -\rangle$ etc. Using (6) and (8) the interacting Hamiltonian, restricted to the states $|\uparrow, \uparrow\rangle, |\downarrow, \downarrow\rangle, |\uparrow, \downarrow\rangle, |\downarrow, \uparrow\rangle, |\uparrow\downarrow, -\rangle$ and $|\downarrow, \uparrow\downarrow\rangle$, is

$$H = E_{0,4m+2} + \begin{pmatrix} -\frac{J}{2} & & & & 0 \\ & -\frac{J}{2} & & & \\ & & 0 & -\frac{J}{2} & \\ & & -\frac{J}{2} & 0 & \\ 0 & & & & u^+ - \varepsilon_\Delta & \frac{J}{2} \\ & & & & \frac{J}{2} & u^+ + \varepsilon_\Delta \end{pmatrix}, \quad (9)$$

with $E_{0,4m+2} = \frac{1}{2} E_c N_c^2 + (2m^2 + 2m + 1)(\varepsilon_0 - u^+) - J(m^2 + m) + 2u^+ m$. Diagonalizing H , we find that its eigenstates are given by the spin 1 triplet $|\uparrow, \uparrow\rangle, |\downarrow, \downarrow\rangle, 1/\sqrt{2}(|\uparrow, \downarrow\rangle + |\downarrow, \uparrow\rangle)$, the spin 0 singlet $1/\sqrt{2}(|\uparrow, \downarrow\rangle - |\downarrow, \uparrow\rangle)$ and the two states $(c_{1/2}^2 + 1)^{-1/2} (c_{1/2} |\uparrow\downarrow, -\rangle \pm |\downarrow, \uparrow\downarrow\rangle)$, where $c_{1/2} = \frac{J}{2} / (\sqrt{\varepsilon_\Delta^2 + (J/2)^2} \pm \varepsilon_\Delta)$. Relatively to $E_{0,4m+2}$,

the eigenenergies are $-J/2$ for the triplet states, $J/2$ for the singlet state and $u^+ \pm \sqrt{\varepsilon_\Delta^2 + (J/2)^2}$ for the remaining two states. Thus, under the condition $J/2 > \sqrt{\varepsilon_\Delta^2 + (J/2)^2} - u^+$, i.e. for a small band mismatch $\varepsilon_\Delta \lesssim J/2$, the ground state is threefold degenerate and formed by the spin 1 triplet, otherwise by $(c_2^2 + 1)^{-1/2} (c_2 |\uparrow\downarrow, -\rangle - |-\rangle, \uparrow\downarrow)$. The low energy spectra for the two cases $\varepsilon_\Delta = 0$ and $\varepsilon_\Delta \gg J/2$ are shown in Fig. 1 for a (6,6) armchair nanotube (corresponding to $d = 0.8$ nm) with an assumed dielectric constant of $\epsilon = 1.4$. The obtained values of $J = 0.09\varepsilon_0$ and $u^+ = 0.03\varepsilon_0$ are in good agreement with the experiments [8, 10], where nanotubes with $\varepsilon_\Delta \gg J/2$ were considered. In accordance with the discussion above, Moriyama et al. [10] could identify the ground state to $N_c = 4m + 2$ as a spin 0 singlet and also a spin 1 triplet was found. Not observed so far has been the spin 1 triplet as ground state and the mixing of $|\uparrow\downarrow, -\rangle$ and $|-\rangle, \uparrow\downarrow)$, as predicted by our calculation for nanotubes with $\varepsilon_\Delta \lesssim J/2$. We emphasize that all the exchange splittings here result from non-forward scattering processes with respect to the band index r . In the considerations of Lieb and Mattis [13] such an additional pseudo-spin degree of freedom is missing and so we conjecture that this is the reason why their theorem can not be applied in our case. The meanfield result of Oreg et al. [12] for the ground state structure to $N_c = 4m + 2$ essentially can be obtained by setting the off-diagonal elements in (9) to zero. Therefore if $\varepsilon_\Delta \gg J/2$, the meanfield approach yields the same ground state spectrum as our work, but with *different degeneracies*: Instead of having a threefold degeneracy of the spin 1 triplet and no degeneracy for the spin 0 singlet, a twofold degeneracy of the states $|\uparrow, \uparrow\rangle$, $|\downarrow, \downarrow\rangle$ and $|\uparrow, \downarrow\rangle$, $|\downarrow, \uparrow\rangle$ respectively, is obtained. Additionally for $\varepsilon_\Delta \lesssim J/2$, the meanfield theory is not capable of predicting the mixing of the states $|\uparrow\downarrow, -\rangle$ and $|-\rangle, \uparrow\downarrow)$ with the accompanying exchange splitting. The ground states of $H_0 + V_{\rho\rho}$ to the charge states $N_c \neq 4m + 2$ do not mix via $V_{n\rho\rho}$ and thus the corresponding energies can be determined easily by using eqs. (6) and (8) for $\vec{N} = \vec{N}'$.

Excitation spectrum So far no bosonic excitations were involved in our ground state examination. In order to discuss the excitation spectrum of $H = H_0 + V_{\rho\rho} + V_{n\rho\rho}$, the matrix elements of $\langle \vec{N}, \vec{m} | V_{n\rho\rho} | \vec{N}', \vec{m}' \rangle$ must be determined. The detailed calculation, based on bosonization techniques, will be given in a longer article [18]. After truncating the Hilbert space at sufficiently high energies and diagonalizing H we obtain for $N_c = 4m + 2$ the spectrum as shown in Fig. 2. For comparison we also show the spectrum of the “standard” theory [1, 5, 11] as obtained by only retaining the dominating forward scattering processes of $V_{\rho\rho}$. Most striking is the partial lifting of the huge degeneracies and the formation of a quasi continuum at higher energies.

In conclusion we have derived a microscopic low en-

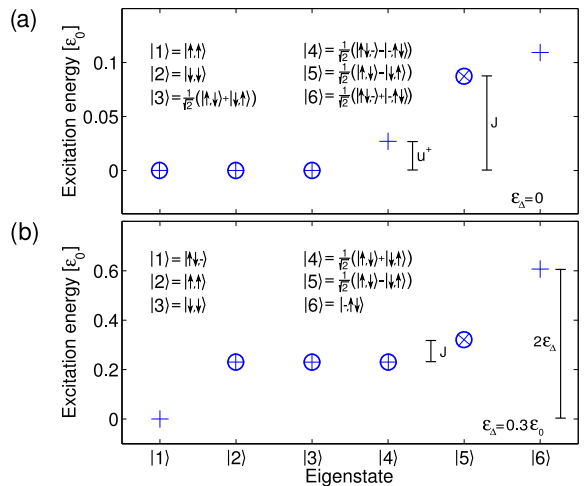


Figure 1: Low energy spectrum of a (6,6) SWNT for $N_c = 4m + 2$. (a) For $\varepsilon_\Delta = 0$ the ground state is formed by the spin 1 triplet ($\rightarrow \oplus$). The states $|\uparrow\downarrow, -\rangle$ and $|-\rangle, \uparrow\downarrow)$ mix. (b) For $\varepsilon_\Delta \gg J/2$ the ground state is given by the spin 0 state $|\uparrow\downarrow, -\rangle$. The spin 0 singlet is indicated by \otimes . The interaction parameters are $J = 0.09\varepsilon_0$, $u^+ = 0.03\varepsilon_0$.

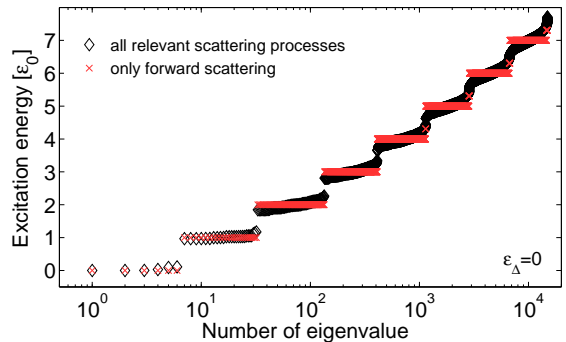


Figure 2: Excitation spectrum of a (6,6) SWNT including only forward scattering processes ($\rightarrow \times$) and for the total Hamiltonian $H = H_0 + V_{\rho\rho} + V_{n\rho\rho}$ ($\rightarrow \diamond$). Note the logarithmic scale of the x-axis. The energy of the lowest $c+$ excitation is $4.3\varepsilon_0$. All other interaction parameters are as for Fig. 1.

ergy theory for finite size metallic SWNTs away from half filling, including non-density-density interaction processes, which become relevant for small diameter tubes. The ground state and excitation spectra have been determined. In particular, we predict a spin 1 triplet as ground state for $N_c = 4m + 2$, if the energy mismatch ε_Δ between the different pseudo-spin branches is much smaller than the exchange energy J , a spin 0 singlet otherwise. For $\varepsilon_\Delta \lesssim J/2$ we furthermore find that the pseudo-spin is not conserved and the corresponding degeneracy is lifted. We notice that in [10] an energy mismatch $\varepsilon_\Delta \gg J/2$ was used to fit the data and, in agreement with our theory, a singlet ground state has been inferred from magnetic field measurements. Observation of the triplet ground

state is within experimental reach.

-
- [1] R. Egger and A. O. Gogolin, Phys. Rev. Lett. **79**, 5082 (1997); Eur. Phys. J. B **3**, 281 (1998).
- [2] H. Yoshioka, A. A. Odintsov, Phys. Rev. Lett. **82**, 374 (1999).
- [3] M. Bockrath *et al.*, Nature **397**, 598 (1999).
- [4] H. W. Ch. Postma *et al.*, Science **293**, 76 (2001).
- [5] C. Kane, L. Balents and M. P. A. Fisher, Phys. Rev. Lett. **79**, 5086 (1997).
- [6] S. J. Tans *et al.*, Nature **386**, 474 (1997).
- [7] D. H. Cobden and J. Nygård, Phys. Rev. Lett. **89**, 046803 (2002).
- [8] W. Liang, M. Bockrath and H. Park, Phys. Rev. Lett. **88**, 126801 (2002).
- [9] S. Sapmaz *et al.*, Phys. Rev. B **71**, 153402 (2005).
- [10] S. Moriyama, T. Fuse, M. Suzuki, Y. Aoyagi, K. Ishibashi, Phys. Rev. Lett. **94**, 186806 (2005).
- [11] L. Mayrhofer, M. Grifoni, Phys. Rev. B **74**, 121403(R) (2006); Eur. Phys. J. B **56**, 107 (2007).
- [12] Y. Oreg, K. Byczuk and B. I. Halperin, Phys. Rev. Lett. **85**, 365 (2000).
- [13] E. Lieb and D. Mattis, Phys. Rev. **125**, 164 (1962).
- [14] For the other types of metallic nanotubes only the magnitudes of the effective 1D interaction potentials change marginally, see, A. A. Odintsov and H. Yoshioka, Phys. Rev. B **59**, R10457 (1999).
- [15] J. Jiang, J. Dong and D. Y. Xing, Phys. Rev. B **65**, 245418 (2002).
- [16] W. Barford, *Electronic and Optical Properties of Conjugated Polymers*, (Clarendon Press, Oxford, 2005).
- [17] For an introduction to bosonization, see e.g., J. v. Delft, H. Schoeller, Annalen Phys. **7**, 225 (1998).
- [18] L. Mayrhofer, M. Grifoni (in preparation).